Appl Phys A (2010) 99: 489–495
DOI 10.1007/s00339-010-5564-9

Applied Physics A
Materials Science & Processing

Effect of annealing temperature on hardness, thickness and phase structure of carbonitrided 304 stainless steel

F.M. El-Hossary · N.Z. Negm · S.M. Khalil · A.M. Abed El-Rahman · M. Raaif · S. Mändl

Received: 21 August 2009 / Accepted: 11 January 2010 / Published online: 24 February 2010

Abstract Carbonitriding of AISI 304 austenitic stainless steel was performed at a plasma-processing power of 450 W using inductively coupled radio frequency (rf) plasma in a gas mixture of 50% N_2 and 50% C_2H_2. The rate of carbonitriding, microhardness, phase structure of the compound layer, surface microstructure and cross-section morphology were studied before and after the annealing process. At the annealing temperature up to 800°C, the microhardness values of the compound zones decrease, while the associated values of the diffused zones increase. Little change was found in the thickness of the compound and diffused zones when the carbonitrided samples were annealed up to 400°C. However, at a higher annealing temperature, the thicknesses of both zones increase. The γ-Fe austenite is the main crystalline phase that can be detected by X-ray diffraction. As the annealing temperature increases up to 500°C, X-ray spectra show α-Fe and Fe_5C_2 phases. Nitrogen diffuses more deeply from the near surface to the interior of the treated sample as the annealing temperature increases up to 800°C and this might explain the extent of carbonitrided thickness and the enhanced microhardness of the diffused zone.

F.M. El-Hossary · N.Z. Negm · S.M. Khalil · A.M. Abed El-Rahman · M. Raaif (✉)
Physics Department, Faculty of Science, Sohag University, Sohag, Egypt
e-mail: mraaif@daad-alumni.de

S. Mändl
Leibniz-Institute für Oberflächenmodifizierung, Permoserstr. 15, 04318 Leipzig, Germany

1 Introduction

Austenitic stainless steels are used in the chemical and food-processing industries. However, their hardness and wear resistance are relatively low. Many attempts have therefore been made to improve the mechanical properties of austenitic stainless steels [1–6]. A new inductively coupled (rf) plasma technique for nitriding [7] and carbonitriding [8] of stainless steel was used which produces a surface layer of exceptional hardness (1800 HV) in extremely short processing time (3 min or longer). The effect of using different plasma-processing time, plasma-processing power, and gases on the properties of 304 stainless steel has been studied elsewhere [9–11]. While usual nitriding and carbonitriding conditions, of stainless steels, have faced comprehensive investigations in the past, very little is still known about the various influences of post-annealing at different temperatures. In this study, experiments were carried out to investigate the effect of different post-annealing temperatures on the carbonitrided 304 stainless steel samples. The thicknesses of the compound and diffused zones, the phase stability and the microhardness values variation are studied.

2 Experimental details

The austenitic stainless steel (AISI) 304 samples consisted of 1 mm thick rolled sheet, cut into pieces with small dimensions of 1.2×2.5 cm^2. The composition of these samples was as follows in wt%: 0.08 Si, 1 Mn, (8-11) Ni, (12-20) Cr, balance Fe and the 304 stainless steel microhardness is 210 HV 0.1. The surface roughness of the used samples was between 100–120 nm. The samples were carbonitrided using radio frequency (rf) plasma inductively coupled operated in continuous mode. The carbonitriding process has been

performed without any pre-treatment for the samples. Details of the carbonitriding system can be found in [10]. In brief, the system is comprised of a quartz reactor with a 500 mm long tube that has a diameter of 41.5 mm and that was evacuated to a base pressure of 2×10^{-2} mbar by a two-stage rotary pump. Nitrogen (N_2) and acetylene (C_2H_2) gas flows were controlled using mass flow meters and a 1:1 pressure ratio was measured. The flow rates were adjusted to establish a gas pressure of 8×10^{-2} mbar, as measured by a capacitance manometer. The induction copper coil, energized by an rf power generator (model HFS 2500 D) at 13.65 MHz via a tunable matching network, generated the discharge. The samples were supported on a water-cooled copper sample holder. The sample temperature was measured during the rf plasma process by a Chromel-Alumel thermocouple, which was placed close to the surface of the sample. The treatment temperature was approximately 475°C. After the carbonitriding process, the samples were allowed to cool slowly in the evacuated reactor plasma tube. The plasma-processing power and the plasma-processing time were fixed to be 450 W and 15 min for all the treated austenitic stainless steel samples.

The as-carbonitrided samples were annealed in a quartz tube under a base pressure of 10^{-2} mbar at temperatures of 100, 200, 300, 400, 500, 600, 700, and 800°C for one hour each. The near-surface structure of the carbonitrided layers was analyzed using a Siemens diffractometer unit with CuK_α radiation. Vickers microhardness measurements of the matrix, as-prepared, post-annealed and the cross-sections of the samples were carried out using a Leitz Durimet microhardness tester with a contact load of 100 gm. The metallographic studies were performed using scanning electron microscopy (SEM) and optical microscopy (OM). Transversally cut sections of the samples were cold embedded in epoxy material. Grinding of the samples was performed using water-proof silicon carbide papers followed by polishing using alumina suspensions. The etching process was performed using 2% nital for 45 s. Finally, the samples were washed and swabbed in warm running water. A micrometer scale attached to the optical microscope measures the thicknesses of the compound and diffusion layers.

3 Results and discussion

3.1 Microhardness measurements

The surface microhardness values of the carbonitrided austenitic stainless steel (CNASS) samples before and after annealing process are shown in Fig. 1. One can observe from this figure that the microhardness of the as-prepared and the post-annealed samples treated up to 300°C have nearly the same value and equal to 1650 HV 0.1, and this represents an 8-fold increase in the surface hardness comparing with the untreated austenitic stainless steel material. Annealing at higher temperatures leads to a gradual decrease in the mi-

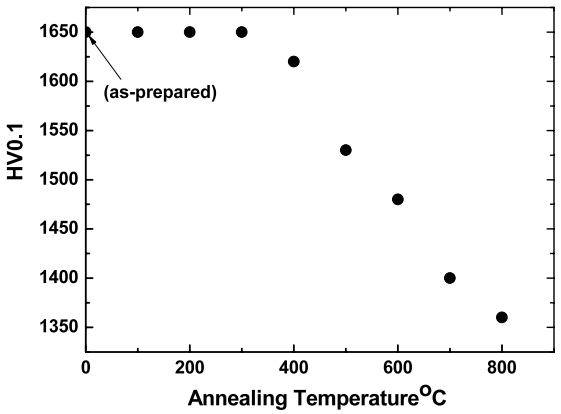

Fig. 1 Surface microhardness values of the as-prepared and post-annealed CNASS samples at different temperatures

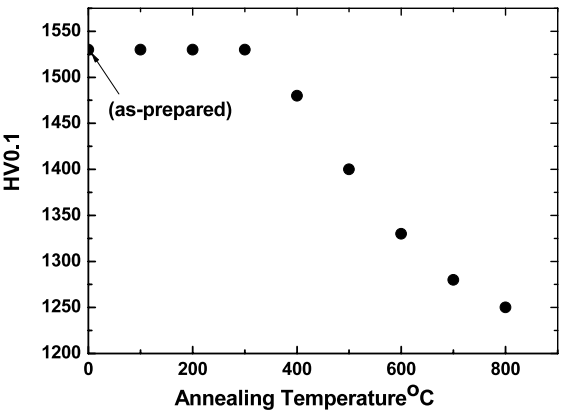

Fig. 2 The microhardness values of the compound layer at 8 μm under the top surface for the as-prepared and post-annealed CNASS samples at different temperatures

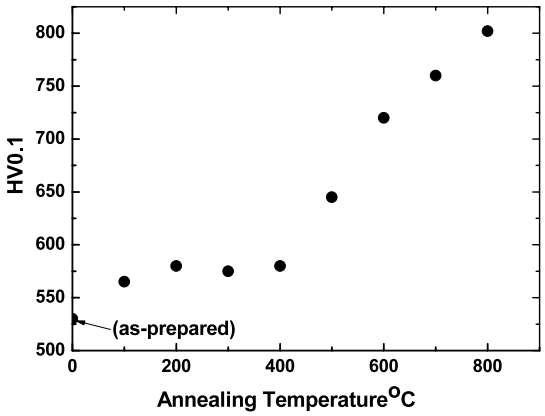

Fig. 3 The microhardness values at the interface between the compound and diffusion zones for the as-prepared and post-annealed CNASS samples at different temperatures

crohardness values of the samples to attain 1360 HV 0.1 for the sample that was annealed at 800°C.

The microhardness profiles for the same above-mentioned samples were measured. The microhardness values of the compound layer at 8 μm under the top surface, at the interface between the compound and diffusion zones, and at the diffusion zone (at 40 and 100 μm under the top surface) are shown in Figs. 2–5, respectively. Figure 2 shows similar microhardness behavior as that shown in Fig. 1. For the effect of annealing temperature on the microhardness values at the interface between the compound layer and diffusion layer, microhardness of behavior opposite to the above, can be clearly observed as seen in Fig. 3. The microhardness has approximately the same value up to 400°C and then increases as the annealing temperatures increase. Moreover, at the diffusion zone (at 40 and 100 μm under the top surface), the microhardness values have the same behavior comparing with the interface between the compound and diffusion zones; this can be seen in Figs. 4 and 5.

3.2 The microstructure of as-prepared and post-annealed samples

The surface morphology of the carbonitrided 304-austenitic stainless steel before and after the annealing process using SEM is shown in Fig. 6. The surface morphology of the untreated austenitic stainless steel (ASS sample) is shown

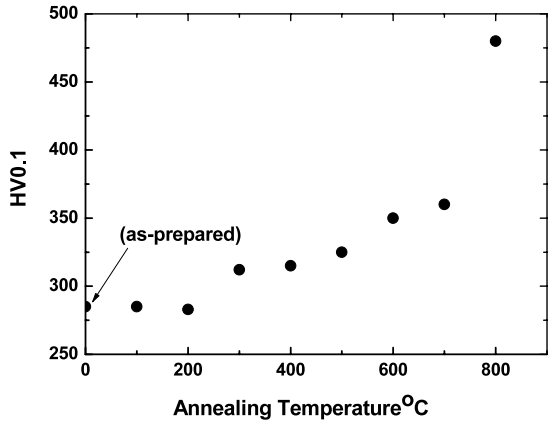

Fig. 4 The microhardness values at the diffusion zone (at 40 μm under the top surface) for the as-prepared and post-annealed CNASS samples at different temperatures

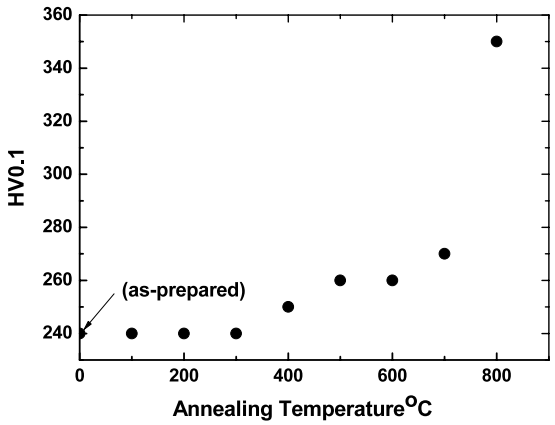

Fig. 5 The microhardness values at the diffusion zone (at 100 μm under the top surface) for the as-prepared and post-annealed CNASS samples at different temperatures

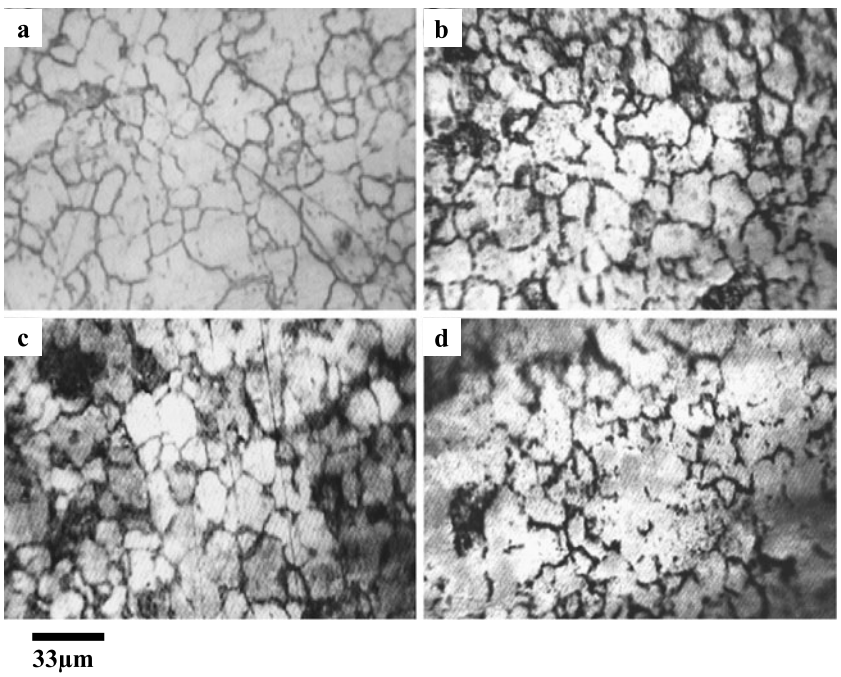

Fig. 6 SEM showing the surface morphology of (**a**) ASS, (**b**) as-prepared CNASS sample treated for 15 min at 450 W, (**c**) post-annealed sample at 400°C, and post-annealed sample at 800°C

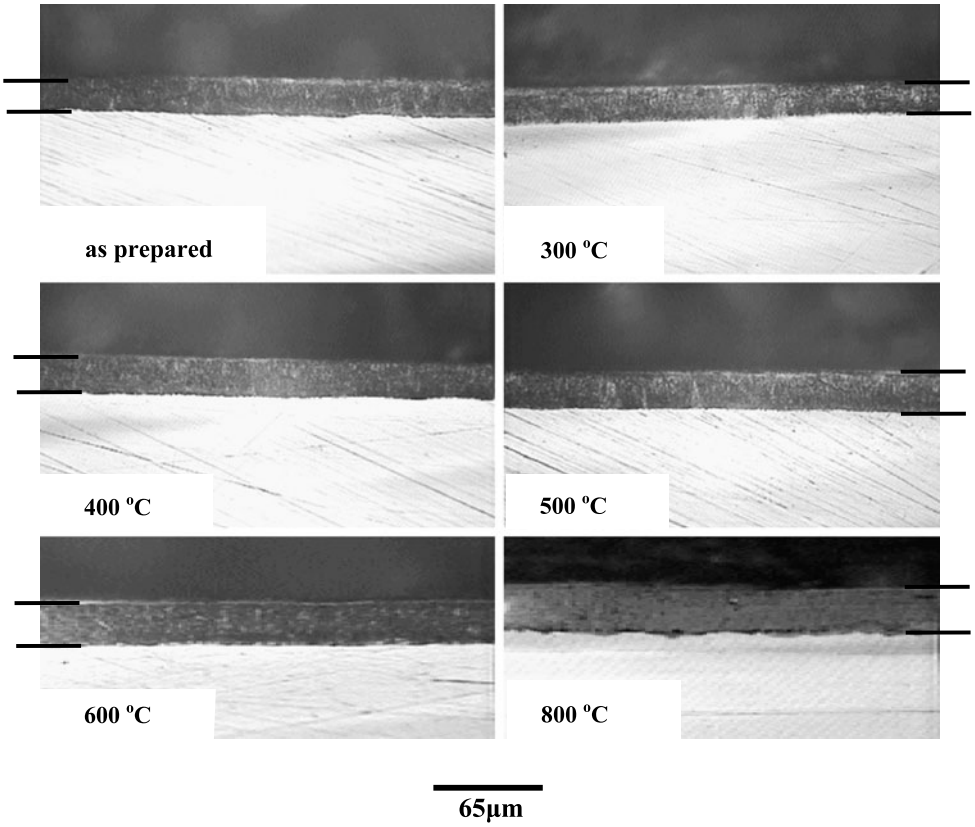

Fig. 7 Optical micrographs showing the cross-section morphology of the as-prepared and post-annealed CNASS samples at different temperatures

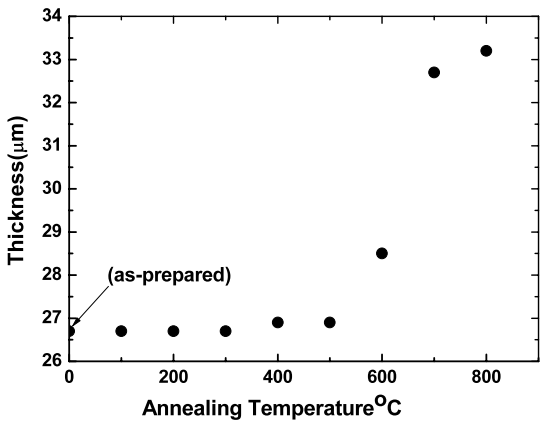

Fig. 8 The thickness of the compound layer for the as-prepared and post-annealed CNASS samples at different temperatures

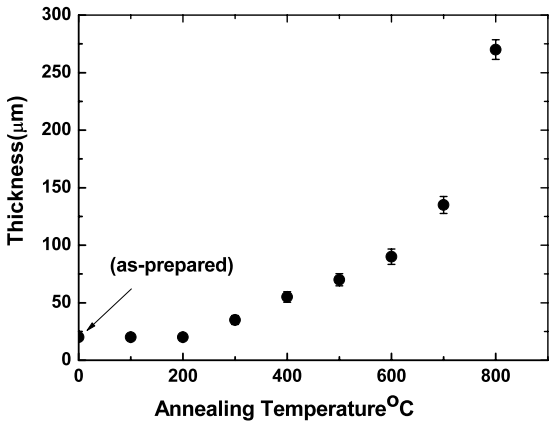

Fig. 9 The thickness of the diffusion layer for the as-prepared and post-annealed CNASS samples at different temperatures

in Fig. 6(a); one can see from this figure that the untreated surface discloses large, non-uniform and randomly packed grains with thin boundaries. Furthermore, undistributed micro-pores have been found on the surface. After plasma carbonitriding of austenitic stainless steel for 15 min at 450 W, the surface is characterized by a smaller grain size and thicker grain boundaries compared to the untreated sample as shown in Fig. 6(b). Moreover, dark precipitations are observed on the grain boundaries, this is related to the chemical compound phase of CrN, these results agree well with [12, 13]. Adding elements such as nitrogen and carbon to the stainless steel matrix is found to have a significant effect on the grain size reduction; moreover, the precipitation of secondary phase like CrN on the grain boundaries is considered to be another factor. The surface morphology, where the granular structure feature is apparently unchanged before and after plasma treatment, indicates that most of the carbonitrided phases which were created during the plasma processing are produced under the surface. The high nitrogen and carbon concentrations in the compound

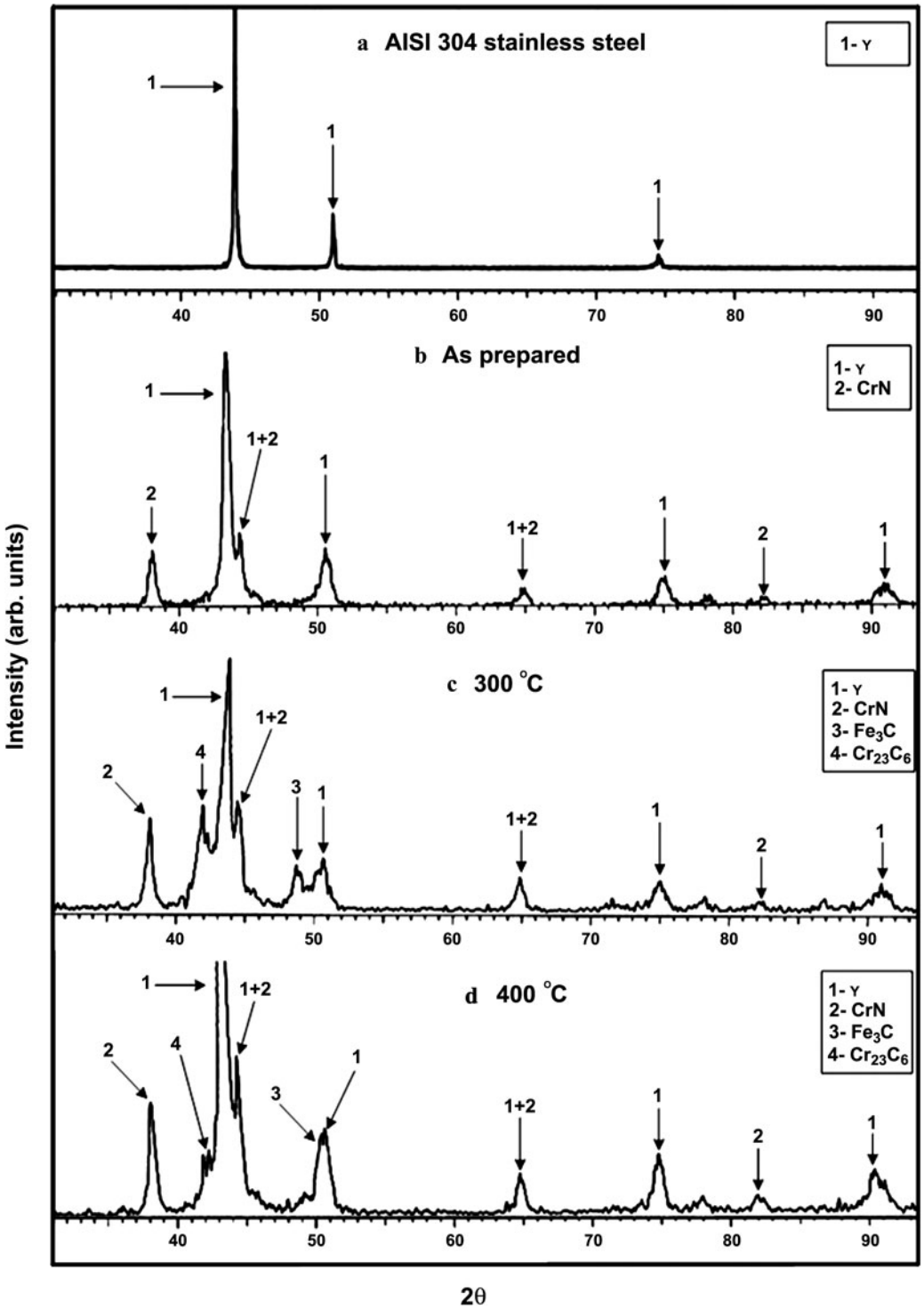

Fig. 10 XRD of the untreated Stainless Steel matrix, as-prepared and post-annealed CNASS samples at different temperatures

layer and the precipitation of phases on the grain boundaries contribute positively to the high microhardness values. For the carbonitrided sample that was post-annealed at 400°C for one hour, no obvious variation in the surface morphology can be observed as seen in Fig. 6(c). In Fig. 6(d), the annealing temperature was high enough (800°C) to rupture most of the grain boundaries.

Optical microscopy was also used to characterize the morphology of the cross-section layers of the CNASS samples before and after annealing processes. The typical cross-

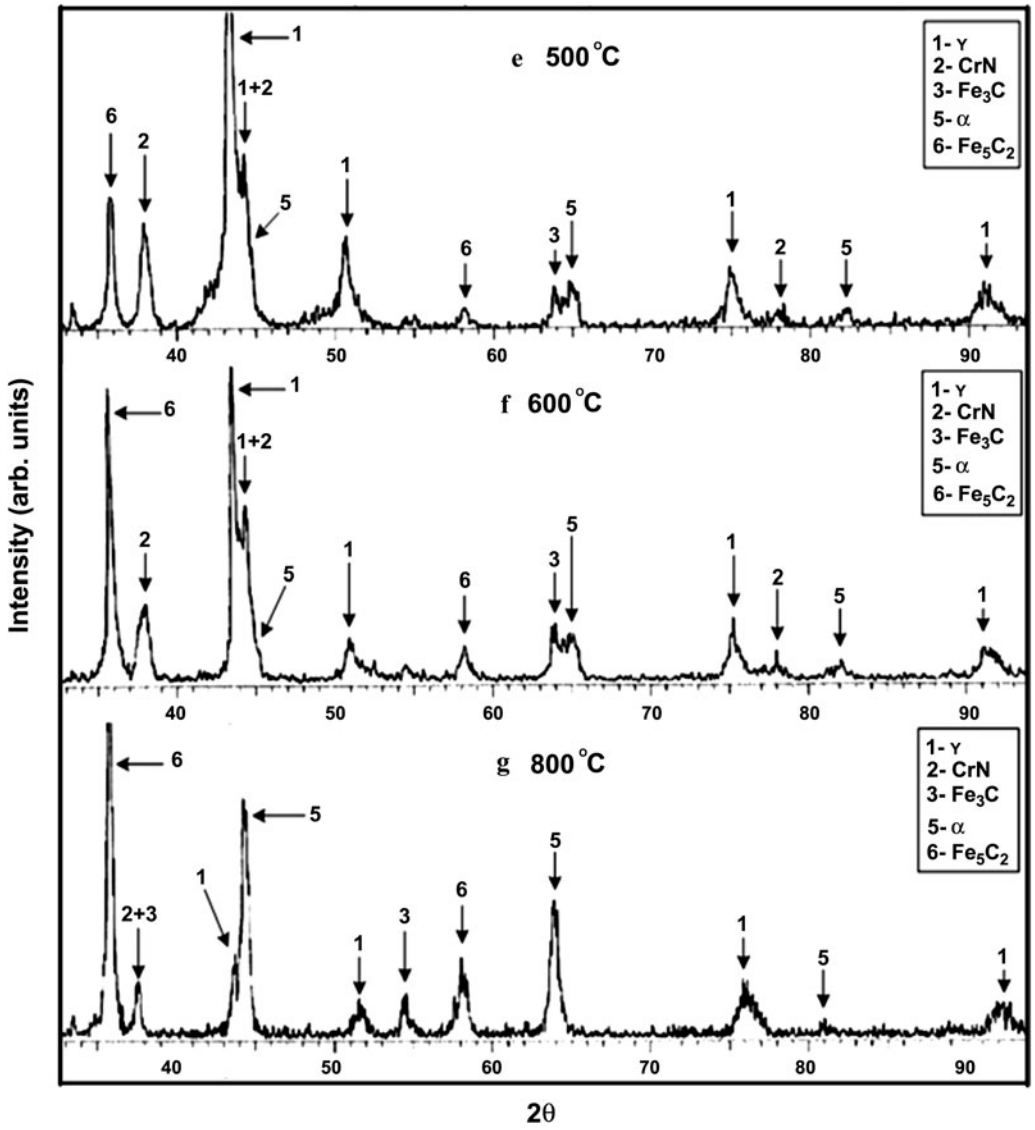

Fig. 10 (*Continued*)

section micrographs of the as-prepared sample carbonitrided for 15 min at 450 W and post-annealed samples at different temperatures are shown in Fig. 7. Examination of the cross-section morphology of the as-prepared and the post-annealed samples up to 500°C reveals the formation of distinct carbonitrided layers with a sharp interface with the bulk material and shows obvious variation in the morphology when the samples are post-annealed at 600 and 800°C. Using a micrometer scale attached to the optical microscope, the thickness of the compound and diffused layers of the samples can be measured. The thickness variation of the compound and diffused zones with annealing temperatures were plotted in Figs. 8 and 9 respectively. In Fig. 8, the thickness of the compound layer is nearly constant and equal approximately 26.7 μm, even for the samples that were annealed up to 500°C. Afterwards, the thickness sharply increases to attain nearly 33 μm for the sample post-annealed at 700°C, followed by slow increase as the annealing temperature increases to 800°C. The diffusion thickness has a more significant thickness variation due to the annealing process as seen in Fig. 9. The underlying diffusion layer of 20 μm (for the as-prepared sample) showed a progressively increased thickness with post-annealing temperature to reach a thickness of 270 μm at 800°C.

The XRD patterns of the untreated Stainless Steel matrix, as-prepared sample carbonitrided for 15 min at 450 W and post-annealed samples at different temperatures are shown in Fig. 10. For the as-prepared sample, the phase distribution shows a high proportion of the native γ-phase and CrN, indicating that C is still in solid solution, thus stabilizing the austenitic γ-phase. In contrast, N has already started to form precipitates, which is the typical behavior observed at a

process temperature of around 400–450°C at a short process time of 15 minutes [14, 15]. Prolonged exposure for 1 hour to an elevated temperature even for 300°C leads to the formation of carbide phases as Fe_3C and $Cr_{23}C_6$ even while no macroscopic mobility (i.e. thickness increase of the compound or diffusion layer) is observed. Increasing the temperature to 500°C resulting in the appearance of α-Fe and Fe_5C_2 phases. The information that more α forms at the expense of γ verifies that, the sample composition is changing due to the moving of nitrogen from the near surface to the depth of the sample. The loosing of nitrogen from the near surface increases as the temperature increases up to 800°C to form principally α-Fe, as shown in the X-ray spectra. At 700°C, the α-Fe phase starts to grow at the expense of γ-Fe. At 800°C the α-Fe becomes more intense than before, but the spectra still contain a considerable proportion of γ-Fe phase. Similar sequence of annealing treatment and X-ray analysis for ASS was made elsewhere [16]. No change in the phase composition (γ-Fe) was found when the sample was annealed up to 600°C.

The above figures show that the annealing temperature up to 300°C does not change the properties of the treated samples. However, obvious variation in the microhardness and little change in the thickness of the compound and diffusion zones can be noticed when the samples were annealed up to 500°C. A remarkable increase in the thickness of compound and diffusion zones can be seen when the samples are annealed up to 800°C. The opposite trend of the microhardness on one side and thickness of compound and diffusion zones on the other give strong evidence to the diffusion of nitrogen/carbon towards the bulk material as the annealing temperature increases. Therefore, the nitrogen/carbon concentrations decrease in the near-surface volume and increase at the interface between the compound and diffused zones with high annealing temperatures. Also, at the diffusion zone the concentration of both nitrogen and carbon increase as the annealing temperature increases. Investigation of nitrogen and carbon concentration profile is under process to confirm this result.

4 Conclusion

AISI 304 austenitic stainless steel sheet was carbonitrided using an inductively coupled radio frequency (rf) plasma using a gas ratio of 50% N_2-50% C_2H_2. Rate of carbonitriding, microhardness, cross-section morphology and phase structure of the compound layer were studied before and after the annealing process. In light of the presented results and discussion, the following main conclusions can be drawn.

(1) With annealing temperatures up to 800°C, the microhardness values of the compound zones decrease while the associated values of the diffusion zones increase.
(2) Little change is found in the thickness of the compound and diffusion zones when the carbonitrided samples are annealed up to 400°C, and with higher annealing temperature, the thickness of both zones increase.
(3) Nitrogen and carbon diffuse from the near surface to the depth of the treated sample as the annealing temperature increases and this might interpret the above conclusions.

References

1. A.P. Tschiptschin, C.M. Garzon, D.M. Lopez, Tribol. Int. **39**, 167–174 (2006)
2. M.J. Boldwin, G.A. Collins, M.P. Fewell, S.C. Kumars, K.T. Short, J. Tendys, Jpn. J. Appl. Phys. **36**(7B), 4941–4948 (1997)
3. J. Baranowska, B. Arnold, Surf. Coat. Technol. **200**, 6623–6628 (2006)
4. D. Manova, S. Maendl, H. Neumann, B. Rauschenbach, Surf. Coat. Technol. **201**, 6686–6689 (2007)
5. M.K. Lei, Y. Huang, Z.L. Zhang, J. Matt. Sci. Lett. **17**, 1165–1167 (1998)
6. B. Skoric, D. Kakas, T. Gredic, Thin Solid Films **317**(1–2), 486–489 (1998)
7. B. Billon, A. Hendry, Surf. Eng. **1**, 125 (1985)
8. F.M. El-Hossary, F. Mohammed, A. Hendry, D.J. Fabian, Z. Szazne-Csih, Surf. Eng. **4**, 2 (1988)
9. F.M. El-Hossary, N.Z. Negm, S.M. Khalil, A.M. Abd El-Rahman, D.N. Mcllory, Surf. Coat. Technol. **141**, 194–201 (2001)
10. F.M. El-Hossary, N.Z. Negm, S.M. Khalil, A.M. Abd El-Rahman, Thin Solid Films **405**, 179–185 (2002)
11. A.M. Abd El-Rahman, F.M. El-Hossary, T. Fitz, N.Z. Negm, F. Prokert, M.T. Pham, E. Richter, W. Moeller, Surf. Coat. Technol. **183**, 268–274 (2004)
12. F. Borgioli, A. Fossati, E. Galvanetto, T. Bacci, Surf. Coat. Technol. **200**, 2474 (2005)
13. J. Flis, J. Mankouski, E. Rolinski, Surf. Eng. **5**(2), 151 (1989)
14. C. Blawert, H. Kalvelage, B.L. Mordike, G.A. Collins, K.T. Short, Y. Jirásková, O. Schneeweiss, Surf. Coat. Technol. **136**, 181–187 (2001)
15. S. Mändl, Plasma Proc. Polym. **4**, 239–245 (2007)
16. F.M. El-Hossary, N.Z. Negm, Appl. Surf. Sci. **181**(3–4), 185–190 (2001)